Portable 543 nm length standard and magnetic-induced zero-crossing shift on length standard transition

Wang-Yau Cheng[a)]
Institute of Atomic and Molecular Science, Academia Sinica, Taiwan, Republic of China
Department of Physics, National Dong Hwa University, Hualien 974, Taiwan, Republic of China

Chun Yi Hu
Department of Physics, National Dong Hwa University, Hualien 974, Taiwan, Republic of China

Jow-Tsong Shy
Department of Physics, National Tsing Hua University, Hsinchu 300, Taiwan, Republic of China

(Received 5 October 2004; accepted 31 January 2005; published online 29 April 2005)

This study reports on the development of a portable iodine-stabilized 543 nm (green) length-standard laser, which is low cost and robust. All the needed optics and electronics were integrated into one box which measured 36 cm in length, 30 cm in width, and 15 cm in height. Simple circuits for third harmonic locking are presented and the laser's frequency instability could be as small as 2×10^{-12}, normalized to one hertz bandwidth. The influence of the magnetic field to the locking point of the 543 nm length-standard transitions was investigated. © *2005 American Institute of Physics.* [DOI: 10.1063/1.1898216]

I. INTRODUCTION

In science, "length standard" refers to the common reference of all length measurements. It is, therefore, crucial to create a convenient and objective length standard for use in both academic and industrial applications. Ever since the velocity of light in a vacuum was defined as 299 792 458 m/s in 1983,[1] atom or molecule-stabilized laser systems have served as the primary length standards.[2] Hence, a handy length standard plays a pivotal role in realizing the definition of meter. Nowadays, 633 nm iodine-stabilized He–Ne laser systems and 532 nm iodine-stabilized Nd:YAG laser systems are the most popular length-standard lasers in the visible region. However, the performance of the former laser system is limited by the configuration of the intracavity iodine cell[3–6] and the aggregate cost of the latter laser system is much higher than that of He–Ne lasers. A compromise must be reached that leads to the ideas of establishing other visible, extra-cavity, and low-cost length-standard lasers, such as iodine-stabilized 543 nm He–Ne lasers.

Iodine-stabilized 543 nm He–Ne laser systems have been the subject of extensive research[7–14] since strong 543 nm absorption was observed in 1986.[15] In 1992, the iodine-stabilized 543 nm laser system was recommended to serve as one of the primary length-standard lasers,[16] and some intercomparisons were held thereafter.[11,14] Therefore, developing a high-stable, low-cost, and robust iodine-stabilized 543 nm He–Ne laser system should be significant in the metrological applications.

In this article, we report on the development of a portable iodine-stabilized 543 nm He–Ne laser. All of the necessary optics and electronics were integrated into one box which measured 36 cm in length, 30 cm in width, and 15 cm in height with the laser's frequency instability as small as 2×10^{-12} (normalized to one hertz bandwidth). The laser system could be routinely frequency locked for more than two days in a noisy environment, and remained locked even when the box was moved.

On the other hand, since more than 35% of the primary length-standard lasers are referred to $^{127}I_2$ hyperfine transitions with percentages that might increase,[17,18] it is crucial to study the influence of the magnetic fields on the locking point of standard transitions. We observed the anomalous Zeeman effect among the 543 nm length-standard transitions, which led to a significant zero-crossing shift of the third harmonic spectrum. We are aware of the possible change of the orbital gyromagnetic constant,[19,20] which is suspected to cause the dramatic change in the spectral features of high rotating iodine molecule.

II. EXPERIMENTAL SETUP

The block diagram of our frequency-stabilized laser system is depicted in Fig. 1, in that a Melles Griot 05-LGR323 laser tube was used onto which a piezoelectric transducer (PZT) tube was glued to modulate the laser frequency and around which a heating tape was wrapped to lock the laser frequency. The laser tube was preheated by heating tape with 1 W power, and was modulated by PZT with 6 MHz optical modulation width (17 MHz/V). The dimension of heating tape was measured as 4 mm wide and 0.2 mm thickness with 11 Ω resistance. It is critical to keep the length of the laser tube from thermal disturbance while still keep the temperature of the laser tube from overheating. Therefore, the following two-stage thermal isolation was used: We enclosed the laser tube into an acrylic box with a small air vent array and shielded the entire system with a 2 mm thick aluminum box. This resulted in a 30 °C (centigrade) thermal equilib-

[a)]Electronic mail: wycheng@pub.iams.sinica.edu.tw

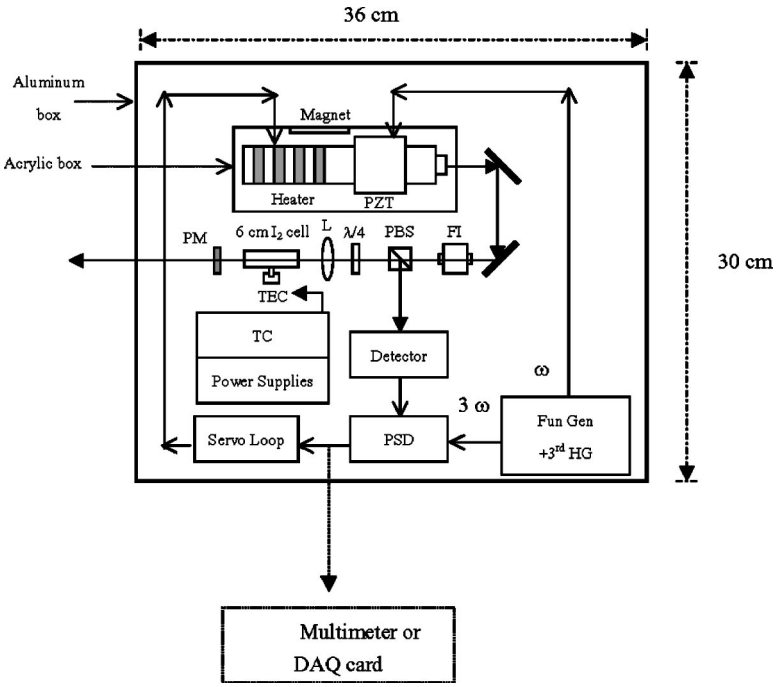

FIG. 1. Block diagram of our portable 543 nm primary length standard system. The laser was enclosed in an acrylic box with a suitable air vent. Here, PZT: piezoelectric transducer; λ/4: quarter wave plate; FI: Faraday isolator; PBS: polarizing beam splitter; *L*: convex lens of focal length 30 cm; PM: 90% partial reflection mirror; SL: servo loop; 31 kHz Gen: 31 kHz sinusoidal wave generator; 3rd HG: third harmonic generator (93 kHz sinusoidal wave); PSD: phase sensitive detector; TC: temperature controller.

rium temperature on the aluminum box at the room temperature of 24±1 °C. Due to the application of a weak magnetic field near the laser tube,[8] the laser output power was found to be about 130 μW with mutually perpendicular two-mode operation for most of the tuning range. As shown in Fig. 1, single frequency was achieved after the Faraday isolator and Doppler-free spectra were obtained via double-pass saturation spectroscopy. The cold finger of the iodine cell was temperature controlled at the recommended 0(±0.003) °C (Ref. 16) by a commercial electronic board[21] which was capable of providing a 12 W output power. Six homemade electronic boards were arranged over the remaining space of the aluminum box as described below:

Figure 2 illustrates the flow chart of our electronics design, in which two ways of the third harmonic generation were presented. One can just use the upper block for generating the third harmonic wave if the needed modulation frequency is high and is fixed. Otherwise, connects the connectors 1, 2 to the lower block labeled as "Frequency variable third harmonic generator," in which the detailed electronics are presented in Fig. 3.

In the upper block (frequency-fixed third harmonic generator) of Fig. 2, an Op-amp relaxation oscillator[22] was built to produce a 186 kHz square wave and was then divided into a 93 kHz square wave and a 31 kHz square wave by four 74LS74N (Dual D-type flip-flop) logic integrated circuits (ICs). Together with adequate bandpass filters, a purified sinusoidal wave was achieved with which the power spectrum to the other harmonics was 55 dB for both the 31 and 93 kHz sinusoidal waves. A typical phase shifter[23] was ap-

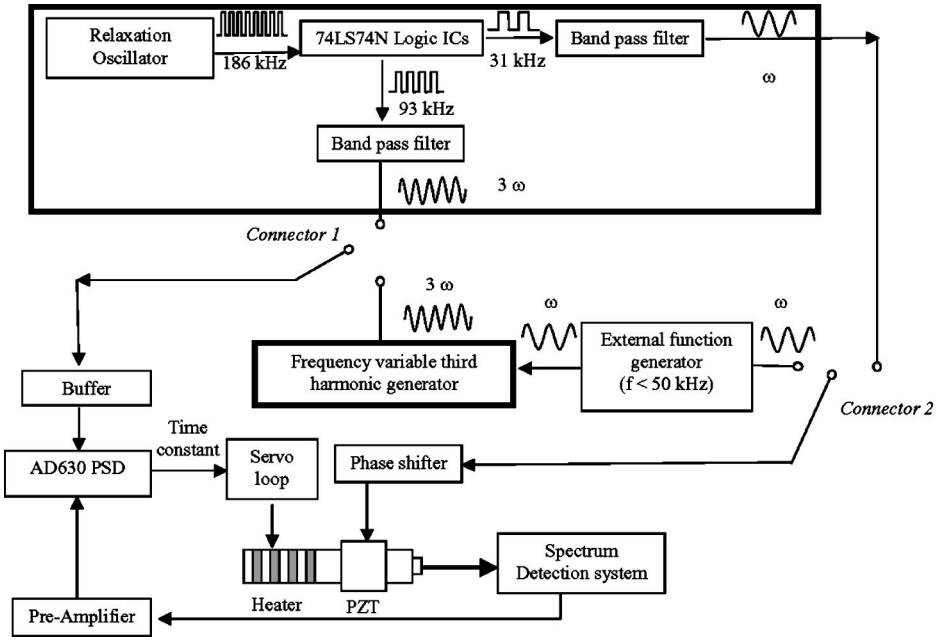

FIG. 2. Flow chart of the electronic design in Fig. 1. PSD: phase sensitive detector. For the third harmonic generators, for higher and fixed modulation frequency, connectors 1, 2, should be connected to the upper block, otherwise, connected to the lower block for arbitrary modulation frequency (<50 kHz). The detailed circuits for lower block are presented in Fig. 3.

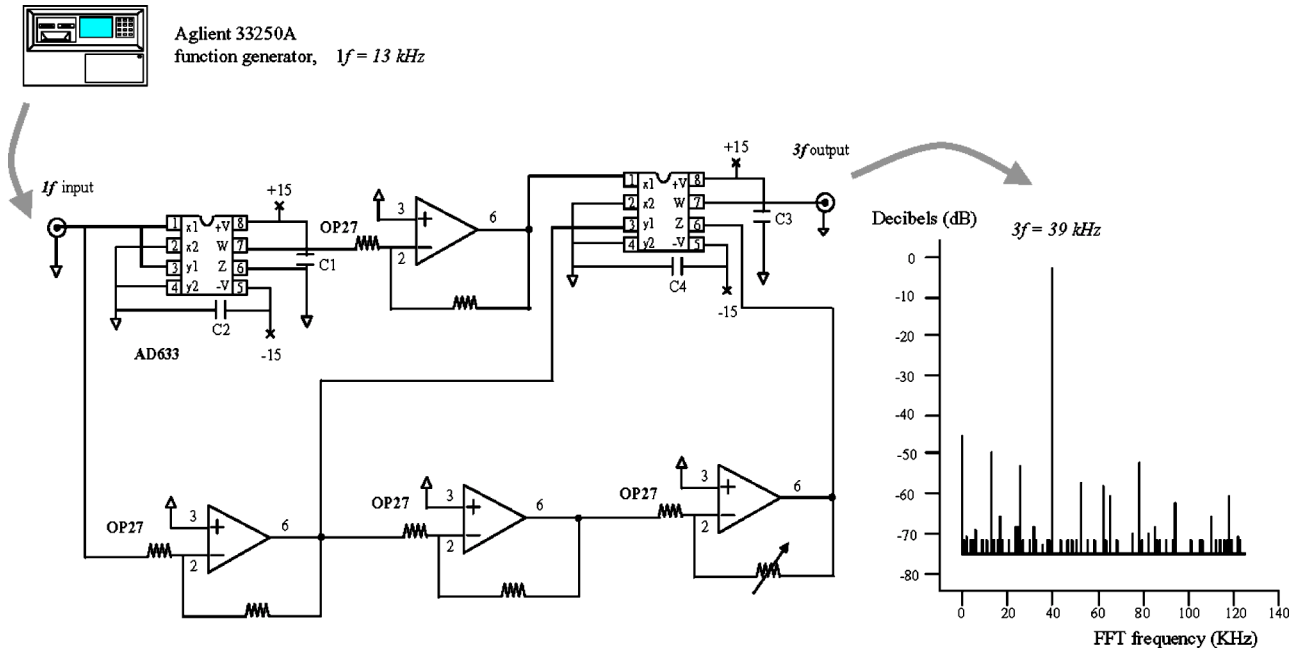

FIG. 3. Simple circuits for a frequency-variable third harmonic generator in Fig. 2. All of the resistors have the same resistance, namely, 10 kΩ, except the adjustable resistor. All of the capacitors have the same capacitance, namely, 0.1 μF. For the 13 kHz testing sinusoidal wave (55 dB harmonic distortion), this circuits get 39 kHz output frequency of near 50 dB harmonic distortion.

plied directly following the output of the 31 kHz sinusoidal wave for modulating the length of PZT tube.

The rest part of Fig. 2 is the lock-in system that is consisted of a high-pass preamplifier, a phase-sensitive detector (PSD, AD630), and an integrator following the output of AD630 for controlling the sampling time constant. The detection system was simply comprised of an (UTD PIN) five-dimensional (5D) photon diode and an Op27 preamplifier. The noise floor of the output of the detection system was 2 mV. A typical proportional-integrator loop circuits, together with a TIP31 power transistor, were used to feedback controlling the current of the heating tape on the laser tube.

The aforementioned circuits were created for the special application of the 31 kHz modulation and 93 kHz demodulation systems, which was tailor made to fit the resonance frequency of our PZT system. In case of external modulation, we switched the connectors 1, 2 to the lower block of Fig. 2. The corresponding electronics are shown in Fig. 3, in which the AD633 ICs play the main role of the frequency tripling. Let *W* denotes the output (pin 7) of the AD633; *X1* (pin 1), *X2* (pin 2), *X3* (pin 3), *X4* (pin 4) denote the four input signals and *Z* (pin 6) denotes the offset voltage, then

$$W = \frac{(X1 - X2)(Y1 - Y2)}{(10V)} + Z. \tag{1}$$

Therefore, by adjusting the gain of the $1f$ signal appropriately as the offset Z of the second AD633, the $3f$ output could be as

$$\sin^3(ft) + \frac{1}{4}\sin(ft) \propto \sin(3ft). \tag{2}$$

The power spectrum of the third harmonic to the other harmonics was above 45 dB with the variable external frequency up to 50 kHz, which was mainly limited by the frequency bandwidth of AD633. The disadvantage of the above circuits is, though not be aware in our experiment, a weakly distorting of the retrieved spectral signal might happen under the 45 dB purification of the $3f$ modulation, that probably shifts the zero-crossing point. Nevertheless, the circuits could be used in all of the experiments requiring the technique of third harmonic demodulation, such as in the laser spectroscopy, NMR detection system, and so on, which benefits the system's overall cost, simplicity and convenience.

The total cost of the aforementioned electronics, including a commercial temperature-control board,[21] was below $700 U.S. dollars.

III. EXPERIMENTAL RESULTS

A. Frequency stability

As shown in Fig. 4, the employment of a 200 kilosample/s data acquisition (DAQ) card revealed a signal-to-noise (SNR) ratio of b_{10} line under 20 ms sampling time.

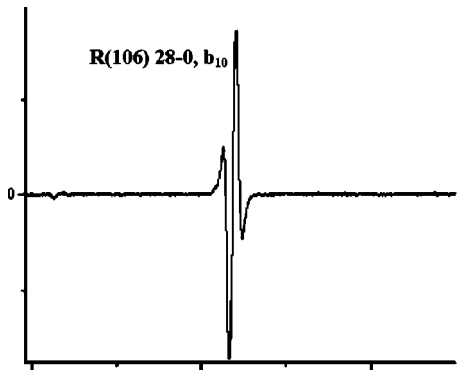

FIG. 4. Signal-to-noise ratio of $R(106)$ 28-0, b_{10} sketched by our portable laser system. Time constant: 20 ms. Modulation width: 6 MHz.

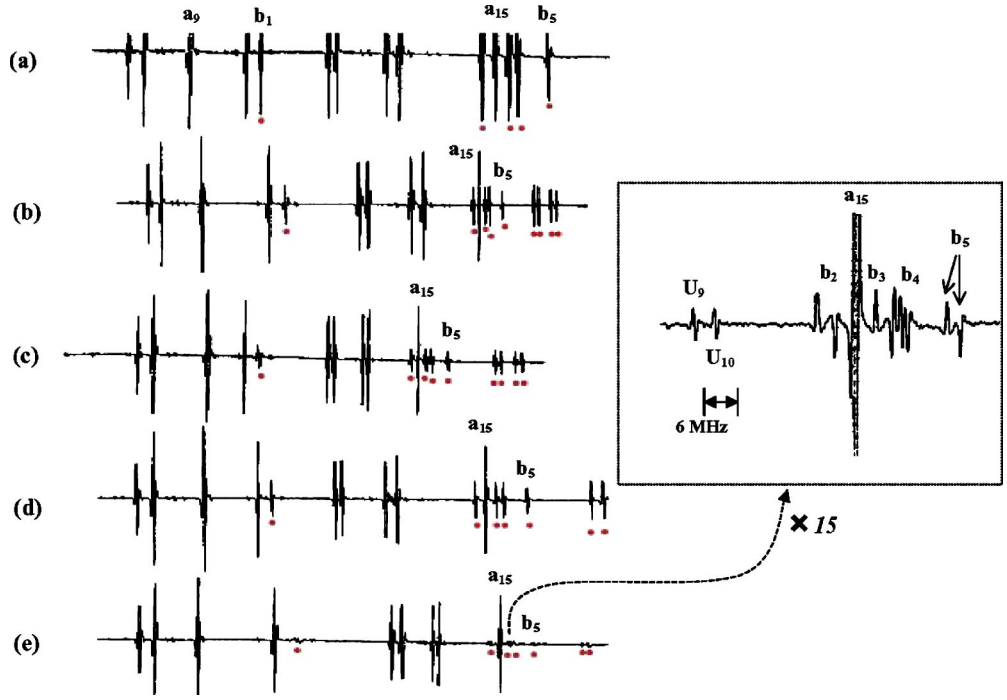

FIG. 5. Spectrum under different magnetic fields. The solid dot under each spectrum indicates the hyperfine transition of $R(106)$ 28-0, while the others are hyperfine transitions of $R(12)$ 26-0. (a) 0 G, (b) 150 G, (c) 300 G, (d) 150 G, (e) 1000 G, where (a), (b), (c), and (e) were recorded under mutual perpendicular linear polarizations of pump and probe beam, respectively, and (d) was that in perpendicular circular polarizations. In (e), the spectrum around a_{15} were magnified and note that the line shape of b lines are abnormal.

When the laser frequency was locked to the b_{10} line, the frequency instability was estimated to as small as 10^{-12} for the sampling time larger than one second. The above instability evaluation is based on our previous studies,[13] in which the relation between the linewidth over the SNR (Δv/SNR) and the Allan variance had been sophisticatedly investigated with the similar laser system. The length standard transition suggested in our previous studies,[13] namely, the b_{10} line, was quite easily found and stabilized due to the comparable short frequency tuning range of He–Ne lasers. The overall system could even be moved without interrupting the frequency locking, which could be kept for more than two days with the other projects being performed on the same optical table.

The offset of the base line was also monitored as we suspected that the box temperature might have changed the offset of the electronics. No obvious offset was found during a one-week observation, during which the box's thermal equilibrium temperature was about 30 °C at 24 °C room temperature.

Note that the aforementioned studies of our frequency-stabilized laser can just show the promising of being a compact, cheap, and robust length standard for the revealed good stability. However, it does not mean that the laser system is already qualified to be a primary length standard since no long-term reproducibility is checked and no intercomparisons of this portable lasers are performed yet.

B. Magnetic-induced zero-crossing shift

As illustrated in Fig. 5, an intriguing spectral feature under weak magnetic field was observed when we applied various permanent magnets transversely to the optical path. We detected a dramatic change of the third harmonic spectra of $R(106)$ 28-0 hyperfine transitions, while the $R(12)$ 26-0 hyperfine transitions remained the same. In Fig. 4(e), the line shape around a_{15} is magnified, where 2 MHz zero-crossing shift of b lines were observed through beating with the other two-mode stabilized green He–Ne laser which instability was 10^{-11} at 1 s sampling time.[24] Similar results were observed for the other $R(106)$ 28-0 hyperfine transitions. Therefore, when one wishes to refer to $R(106)$ 28-0 hyperfine transitions as being a primary length standard, a shielding of the magnetic field is advised. On the contrary, no change was found for the other $R(12)$ 26-0 transitions under our measurement resolution. (See Fig. 5.)

There are two possible reasons for the spectral changes: One reason is that the spin-orbit coupling model is not adequate in the case of a high rotation quantum number. The other reason is that the line shape was broadened by the slightly change of nuclear gyromagnetic constant (which will be defined later) during one photon transition and this effect is amplified by high rotational quantum number. Here we suspect the latter reason since no report was found on determining the hyperfine constants using the spin-orbit decoupled model.[25,26] Therefore, if the latter reason is possible, we estimate here the possible change of a nuclear gyromagnetic constant by observing the zero-crossing shift caused by the superposition of the dense anomalous Zeeman splittings that the corresponding transition frequency can be written as[19]

$$(v_0 + \Delta v) = (H_0 + H')/h = [H_0 - (\mu_n g_i' \vec{I} + \mu_n g_j \vec{J})\vec{B}]/h$$
$$= [H_0 - \mu_n g_{if} m_z B]/h \quad (3)$$

where the

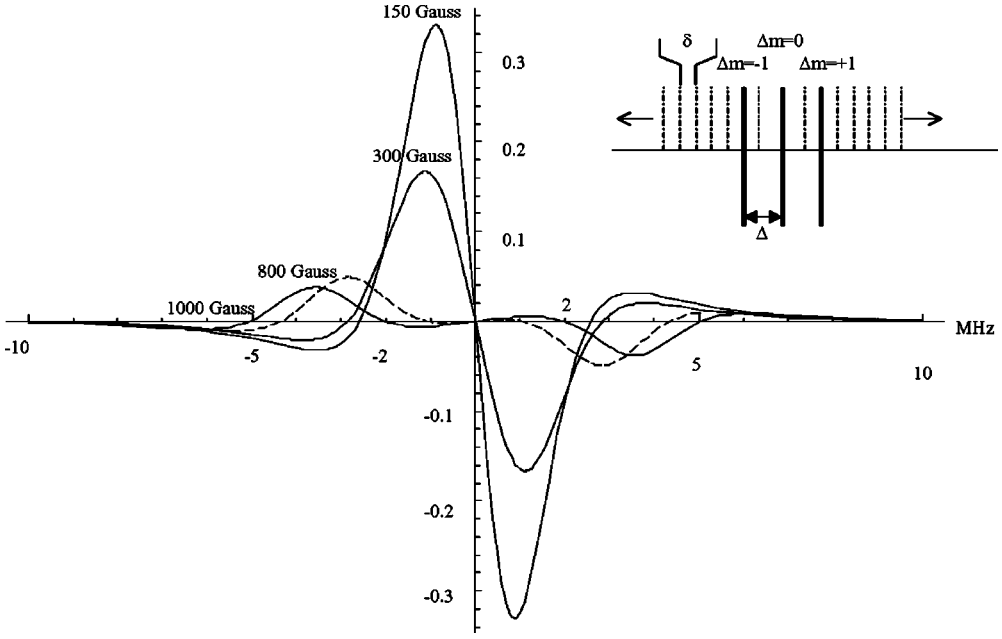

FIG. 6. Simulation results under different magnetic fields, in which the amplitudes are normalized to a zero magnetic field. Here, $g_j'=-0.1576$ and $g_j''=-0.1158$ were employed; thus, $\Delta=80.59$ kHz and $\delta=32.35$ kHz were obtained under a 1000 G magnetic field (Δ, δ, see text).

$$g_{if} = g_i'\beta + g_j(I-\beta), \tag{4}$$

$$\beta = [F(F+1) + I(I+1) - J(J+1)]/2F(F+1), \tag{5}$$

μ_n is the nuclear magneton; $\vec{I}$ is nuclear spin; $\vec{J}$ is orbital angular momentum; $\vec{F}=\vec{J}+\vec{I}$ is the total angular momentum; and m_z is the projection of $\vec{F}$ onto the magnetic field direction of $\vec{B}$ and the nuclear gyromagnetic constant

$$g_i' = g_i + g_1 \tag{6}$$

with $g_i=1.123$ (Ref. 19) and g_1 is the screen effect by electrons, whose value changes below 10% of g_i' at different rovibronic quantum states.[19] In general, $g_1 \ll g_i$ when orbital angular moment $\vec{J}$ is large.[19]

In Fig. 6, the frequency splitting is depicted in which

$$\delta = \mu_n B\Delta g/h = \mu_n B(g_{if}' - g_{if}'')/h, \tag{7}$$

$$\Delta = \mu_n B g_{if}'/h, \tag{8}$$

with g_{if}' standing for the upper level and g_{if}'' standing for the lower level.

In general, δ and Δ are minimal values since iodine molecules are homonuclear molecules whose magnetic dipole is low by nature. Therefore, the anomalous Zeeman effect was not easily detected under a weak magnetic field. Notwithstanding, for high rotating molecular iodine, $(2F+1)^*\delta$ could possibly be even larger than the linewidth if $g_j'-g_j''$ might not trivially be treated the same. For example, for the $R(106)$ 28-0 b_5 line, namely, $F=111$ and I=4 hyperfine transition, the frequency separating under magnetic field can be expressed as

$$\delta = [-0.000\,280\,45 + 0.7348(g_j' - g_j'') + (0.036\,036 g_1' - 0.036\,363\,6 g_1'')]^* B \tag{9}$$

and

$$\Delta = [0.030\,85 + 0.0275 g_1' + 0.7346 g_j']^* B, \tag{10}$$

where δ, Δ are in megahertz and B is in gauss; g_j', g_1' is for the upper level and g_j'', g_1'' is for the lower level. Figure 6 shows the line-shape simulation from a weak magnetic field to a strong magnetic field, where $g_j'=-0.16$ and $g_1'=-0.15$ were adopted from the tendency of Ref. 19. Since δ and Δ are small numbers ($\sim$32 and 81 kHz, respectively) in comparison with the linewidth ($\sim$6 MHz), the zero-crossing shift is thus mainly due to the linewidth broadening caused by $(2F+1)^*\delta$. Note that, since 0.74 is one order larger than 0.036 in Eq. (7), the effect of g_j variation dominates rather than g_1. In other words, for the higher rotational quantum number, the zero-crossing shift was sensitive to $\Delta g_j = g_j' - g_j''$. Therefore, zero-cross fitting offers a way to ascertain the Δg_j and it was fitted as 0.043 in our case. This value was not precise, since the magnetic field was not homogenous enough; however, under the noticeable zero-crossing shift and from the formula of δ, one can conclude that g_j' might not be considered to be the same as the g_j''. Note that this simple analysis could not provide the generality for all hyperfine transitions of iodine molecule, especially for the transitions which energy level higher than the pre-dissociation region.[26]

Another advantage of this rotational-level dependent spectrum over the regular spectrum is that offers a quick way for the preliminarily checking of unknown dense sub-Doppler transitions of iodine molecules. For example, we also discovered that the unknown transitions, namely, u_3, u_5, u_6 in Ref. 12, disappear under a strong magnetic field, while the seven other unknown transitions remained the same. This indicates that the unknown transitions do not belong to the same rotational levels, more precisely, u_3, u_5, u_6 should belong to the transitions of higher rotational quantum number, such as the weak $P(110)$ 35-2 transition.

ACKNOWLEDGMENT

The authors wish to extend their appreciation to the National Science Council of R.O.C. under Contract Nos. NSC 92-2112-M-249-017 and NSC 92–2112–M-001–054 for supporting this project.

[1] Documents concerning the new definition of the meter, Metrologia **19**, 163 (1984).
[2] T. J. Quinn, Metrologia **30**, 523 (1994), and references therein.
[3] M. Erin, B. Karaboce, I. Malinovsky, A. Titov, H. Ugur, H. Darnedde, and F. Riehle, Metrologia **32**, 301 (1995/96).
[4] J.-M. Chartier and A. Chartier, Metrologia **34**, 297 (1997).
[5] B. Stahlberg, B. Ikonen, J. Haldin, J. Hu, T. Ahola, K. Riski, L. Pendrill, U. Karin, J. Henningsen, H. Simonsen, A. Chartier, and J.-M. Chartier, Metrologia **34**, 301 (1997).
[6] V. Navratil, A. Fodrekova, R. Gata, J. Blabla, P. Balling, M. Ziegler, V. Zeleny, F. Petru, J. Lazar, Z. Vesela, J. Gliwa-Gliwinski, J. Walczuk, E. Banrti, K. Tomanyiczka, A. Chartier, and J.-M. Chartier, Metrologia **35**, 799 (1998).
[7] J.-M. Chartier, S. Fredin-Picard, and L. Robertsson, Opt. Commun. **74**, 87 (1989).
[8] H. Simonsen and O. Poulsen, Appl. Phys. B: Photophys. Laser Chem. **50**, 7 (1990).
[9] U. Brand, Opt. Commun. **100**, 361 (1993).
[10] T. Lin, Y.-W. Liu, W.-Y. Cheng, J.-T. Shy, B.-R. Jih, and K.-L. Ko, Opt. Commun. **107**, 389 (1994).
[11] H. R. Simonsen, U. Brand, and F. Riehle, Metrologia **31**, 341 (1995).
[12] W.-Y. Cheng, J.-T. Shy, and T. Lin, Opt. Commun. **156**, 170 (1998).
[13] W.-Y. Cheng and J.-T. Shy, J. Opt. Soc. Am. B **18**, 363 (2001).
[14] H. R. Simonsen, J. Hu, and K. Nyholm, Metrologia **37**, 709 (2000).
[15] J.-M. Chartier, J. L. Hall, and M. Glaser, *Proceedings CPEM'86*, 23 June 1986, p. 323.
[16] T. J. Quinn, Metrologia **30**, 523 (1993/1994).
[17] T. J. Quinn, Metrologia **40**, 103 (2003).
[18] W.-Y. Cheng, L. Chen, T. H. Yoon, J. L. Hall, and J. Ye, Opt. Lett. **27**, 571 (2002).
[19] M. Broyer, J.-C. Lehmann, and J. Vigue, J. Phys. A **36**, 235 (1975).
[20] A. N. Goncharov, S. V. Gateva-Kosteva, M. N. Skvortsov, and V. P. Chebotayev, Appl. Phys. B: Photophys. Laser Chem. **52**, 311 (1991).
[21] Wavelength electronics HTC-1500.
[22] P. Horowitz and W. Hill, *The Art of Electronics*, 2nd ed. (Cambridge University, New York, 1989).
[23] D. F. Stout, in *Handbook of Operational Amplifier Circuit Design*, edited by M. Kaufman (McGraw-Hill, New York, 1976).
[24] W.-Y Cheng, Y.-S Chen, C.-Y Cheng, J.-T Shy, and T. Lin, Opt. Quantum Electron. **32**, 299 (2000).
[25] C. H. Townes, *Microwave Spectroscopy* (Dover, New York, 1975), Chap. 6.
[26] There are numerous papers worked on determining the hyperfine constants of iodine molecular, especially the works related to length standards in 500–543 nm, 612, 633, 640 nm wavelength, and so on. For example, L. Chen, W.-Y. Cheng, and J. Ye, J. Opt. Soc. Am. B **21**, 820 (2004).